A Hybrid FEM/BEM Approach for Designing an Aircraft Engine Structural Health Monitoring

S.C. Forth[1] **and A. Staroselsky** [2]

Abstract: A new hybrid surface-integral-finite-element numerical scheme has been developed to model a three-dimensional crack propagating through a thin, multi-layered coating. The finite element method was used to model the physical state of the coating, and the surface integral method was used to model the fatigue crack growth. The two formulations are coupled through the need to satisfy boundary conditions on the crack and external surface. The coupling is sufficiently weak that the surface integral mesh of the crack surface and the finite element mesh of the uncracked volume can be set up independently. Thus, when modeling crack growth, the finite element mesh can remain fixed for the duration of the simulation as the crack mesh is advanced. This method was developed to evaluate the feasibility of fabricating a structural health monitoring system for real-time detection of surface cracks propagating in aircraft engine components. In this work, the authors formulate the hybrid surface-integral-finite-element method and discuss the mechanical issues of implementing a structural health monitoring system in an aircraft engine environment.

keyword: hybrid numerical method, health monitoring, finite element, boundary element, aircraft engine, crack propagation

1 Introduction

The objectives of this paper are two-fold. The first objective is to present a new efficient numerical method to study the propagation of spatial nonplanar cracks in non-homogeneous media. The second objective is to apply this numerical tool to the engineering problem of monitoring the structural health of safety critical aircraft engine parts and develop design recommendations.

[1] NASA Langley Research Center, 2 West Reid St., MS 188E, Hampton, VA, U.S.A.

[2] United Technologies Research Center, 411 Silver Lane, East Hartford, CT, U.S.A

The failure of safety critical aircraft engine parts, for instance, fan, compressor, and turbine disks, can have catastrophic consequences, see Curley, Fisher, Dileonardi and DePinho (1996). Therefore, implementing a light-weight in-situ sensor system capable of detecting impending failures would allow timely maintenance actions leading to an increase in overall aircraft safety. There are a number of research publications on in-situ sensor methods for rotating, high-temperature equipment based on the eddy current method, see Barranger (1984) and Fahr, Chapman, Pelletier and Hay (1997). However, these approaches are typically unable to physically monitor a large surface, the diagnostic signals gradually degrade with time, and long-term histories must be stored and analyzed, see Tietze (1990). To address these limitations, a new crack sensor system must be defined that would function at a high temperature and not require the on-board data storage requirements of current systems.

To address the above requirements, a sensor architecture was chosen that combines previous work in thin film high temperature sensors with various methods of remotely sensing changes in the electrical properties of conductive strips or wires. The sensor system consists of a conductive material mesh (*e.g.* metal wire) coated onto the rotating engine part, using an alumina bond. The sensor system works by detecting a change in the electrical impedance of the mesh due to wire breakage caused by rotating engine part surface cracks. Therefore, the critical design issue is to predict the subsurface/surface crack propagation throughout the sensor wires. A fracture mechanics study needs to be performed to predict the mechanical and fracture performance of the coating system.

The fatigue crack propagation in a thinly coated part is a difficult mathematical and mechanical problem. Wire properties differ from the characteristics of the surrounding coating and substrate material. Therefore, a crack propagating from the substrate might, and in many cases would, change its trajectory and delaminate the sensor. Subsequently, in such a scenario, the sensor signal would

not be sent. The practical purpose of this paper is to identify loading conditions and sensor geometries that would allow the crack, initially embedded in the rotating engine part, to propagate through the wire without causing sensor delamination.

Study of the mechanics of short fatigue crack growth is fundamental to both structural health monitoring and improved material design. Although a large body of literature that is devoted to the mathematical aspects of crack propagation based on calculation of local stress intensity factors (SIF) exists, very little is known about general non-planar subsurface crack propagation and stability. Despite the significant advantces in analytical technique, only problems with relatively simple geometries could be analyzed in three dimensional formulations. Spatial crack analysis presents a real challenge even for static problems, consequently a limited number of complete solutions are known for arbitrary shaped cracks. Furthermore, the solution of crack problems are even more difficult in the vicinity of free surfaces and interfaces. As soon as the crack tip approaches a bi-material interface, the strength of the stress singularity changes and further crack behavior significantly differs from homogenious media. All the above dictates the requirement for numerical study. In this work, the authors develop a computational fracture mechanics model and apply this technology to identify the requirements for an in-situ crack sensor system that could withstand the aircraft engine operating environment.

The outline of the paper is as follows. In section 2 we address the requirements for and propose a new sensor system based on recent advances in thin film technologies. In section 3 we set down the theoretical formulation of the hybrid numerical method. In section 4 we verify the accuracy of the method by comparing the results to a number of known literature problems. In the fifth section we mathematically formalize the crack sensor problem, and apply the hybrid method for the analysis of crack propagation through the system substrate-multi-layered sensor. We investigate possible regimes of crack instability and sensor delamination. Based on the results of the numerical analyses, we make some practical recommendations for crack sensor design. We close in Section 6 with some final remarks.

2 Aircraft Engine Sensor Requirements

An in-situ sensor system designed for high-temperature, rotating applications must conform to the following physical requirements (a schematic of an engine component and proposed sensor placement is shown in Figure 1):
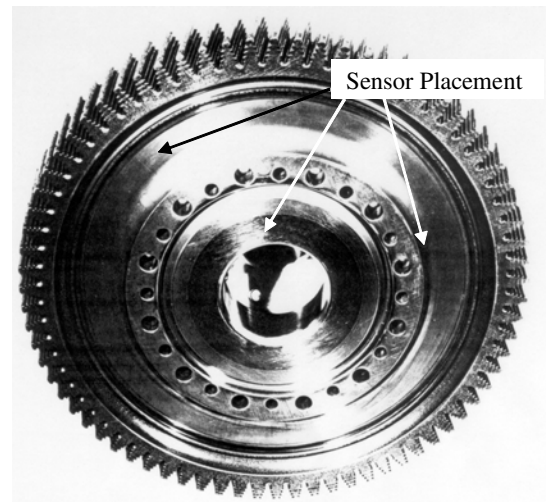
Figure 1 : Component schematic and sensor placement location.

- sensor cannot add significant weight to the structure

- sensor must sense impending component failure without "false alarms" due to FOD, light impact or manufacturing damage.

- coefficient of thermal expansion cannot vary significantly from the base material

- bond for an attached sensor must be able to withstand the thermal expansion of the component and the physical stress of rotation

- sensor must require little user interaction or local data storage

- sensor must not interfere with the continual operation of the engine

- sensor must be cost-effective and readily applicable in a manufacturing environment

- sensor must have tolerances consistent with component design

2.1 Thin Film Sensor

Evaluation of current nondestructive inspection methods and the sensor requirements listed in the introduction leads to a sensor design based on thin-film technology. Thin films add little mass to the structure due to small volume; are designed for use in high temperature environments; and can be deposited on an existing structure within current manufacturing tolerances, see Auciello (1999). Choosing the proper material will enable the thin film to act as an electrical device for sensing systems; absorb impact damage from FOD; and be less susceptible to corrosion than the base component, see Elshabini-Riad and Barlow (1998). Recent research in thin film sensors, as described by Lei, Martin and Will (1997), points to tailoring the material properties, such as electrical impedance, to fit the application. The authors further consider a sensor system, which operates by detecting a change in the electrical impedance of a conductive mesh due to mechanical changes caused by surface and subsurface cracks. Of the electronic concepts the wireless/magnetic coupling approach has been demonstrated in the laboratory with a physical vapor deposited coating, including a 50 μm alumina insulating layer on a metallic substrate. A drawback of this approach is the requirement for an excitation coil and a receiver coil, which are in close proximity to the disk surface. Limitations on the placement of these coils, as well as adapting them for the elevated temperature environment, have not yet been studied.

2.2 Sensor Damage Tolerance

A damage tolerant approach was taken to design the sensor system. First, the sensor must be attachable to the component (shown in Fig. 1). Thin film technology has developed a means of vapor deposition that deposits the coating on rough surfaces with favorable delamination properties, see Metev (1998). The coating must also be within a given tolerance of the coefficient of thermal expansion (CTE) of the component. If the CTE is significantly different from that of the component, then the thermal cycling of the engine during operation will cause the sensor to delaminate. An idealized loading and temperature spectrum are shown in Figure 2. A simple way of determining if this phenomenon will occur is to assume the bond between the coating and the component behaves according to macroscopic fracture mechanics, see Dharan (1986). If the stresses reach the point that
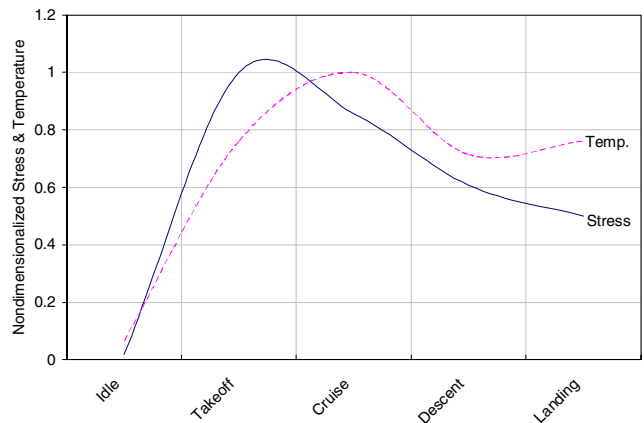

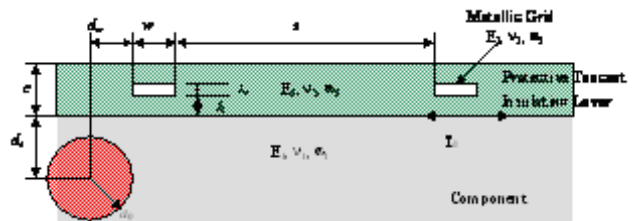**Figure 2** : Idealized loading and thermal sequence.

Figure 3 : Definition of crack sensor system (cross section).

a rogue void's, or crack's, stress intensity factor exceeds the local fracture toughness for the bond, then delamination occurs. Also, since the component is rotating, the centrifugal forces of the component must not cause the sensor to delaminate. The sensor system is designed to generate a signal when a crack of a given size is in the base component. The sensor will consist of at least three layers deposited sequentially onto the surface of the component, as shown in 3. The variables are defined such that: a_0 is the initial crack radius, c is the thickness of the coating, d_c is the distance from the crack to the coating, s is the distance between wires, d_w is the distance from the crack center to a wire ($0.5\ s$), h is the height of the wire from the base material, t_w is the thickness of the wire, w is the width of the wire, K_{T1} is the fracture toughness of the base material, K_{Td} is the delamination fracture toughness of the sensor/base material bond (assumed to be $0.195\ K_{T1}$), E_1, ν_1, α_1 are the Young's modulus, Poisson's ratio and coefficient of thermal expansion for the base material, E_2, ν_2, α_2 are the material properties of the coating and E_3, ν_3, α_3 are the material

properties of the wires.

3   Formulation of Numerical Method

The numerical methods available for crack analysis are mostly limited to finite elements (FEM) and boundary elements (BEM). For decades the FEM has been extensively used for solving fracture mechanics problems. However it is not efficient for problems with singularities because a fine mesh is needed near the crack front. BEM, see Brebbia (1978), has also been widely used in continuum mechanics. It reduces the order of the problem and is well suited for problems with singularities, see Keat, Annigeri, and Cleary (1988). However, the system matrix is full and unsymmetrical, so if used to model large geometries, the BEM is also computationally expensive.

The combination of the boundary and finite element methods to model a cracked structure has been achieved in two- and three-dimensions, such as Annigeri, Keat and Cleary (1988) and Han and Atluri (2002 and 2003) and Cruse (1988). The hybridization of the boundary to finite element method is attractive because the boundary element method provides a very fast, simple solution to modeling the singularity of a cracked structure and the finite element method provides a very robust solution to modeling a complex structural entity, such as in Shifrin and Staroselsky (2002) and Atluri (2005). This coupling is accomplished via a pairing of the boundary conditions of the two methods. The correction vector of boundary loads due to a crack can be expressed as a linear combination of crack traction forces, which, in turn, are a linear combination of external boundary conditions. Thus,

linear superposition allows coupling of both (FEM) and (BEM) methods into one block matrix equation.

The surface integral method, an indirect boundary element method, has been combined with the commercial finite element program NASTRAN to form the hybrid solution. The PATRAN user interface is used for defining the finite element model and the boundary conditions of the surface integral method. The following sections will describe the hybridization of the methods and a detailed explanation of the surface integral method. The discussion of NASTRAN will be cursory since it is commercially available software.

3.1   Boundary and finite element hybridization

Combining the boundary and finite element methods has been accomplished through coupling the boundary conditions of the two models. The crack problem in a finite body is linearly decomposed to a boundary value problem for the finite continuous body and to a crack problem in an infinite region as shown in 4. Additional coupled traction and loading corrections appear on the crack and external surfaces. Crack traction $\{T^c\}$ is the stress that is generated along the imaginary crack surfaces in a continuous body due to the boundary conditions (R and T). Subsequently, the new traction vector applied to the crack should be $\{T - T^c\}$. Similarly, the load correction vector $\{-R^c\}$ accounts for the stresses on the imaginary outer boundary in the finite body due to crack traction. 2 graphically depicts this coupling through linear superposition as described above.

Mathematically, this coupling can be expressed in the finite element equation relating displacement to stress such that

$$[K]\{U\} = \{R\} - \{R^c\} \tag{1}$$

where $[K]$ is the finite element stiffness matrix, $\{U\}$ is the vector of finite element nodal displacements, $\{R\}$ is the external nodal load vector, and $\{R^c\}$ is introduced to the equation to satisfy the external traction boundary conditions that are not enforced in the surface integral model.

The boundary element problem is described by the singular integral equation
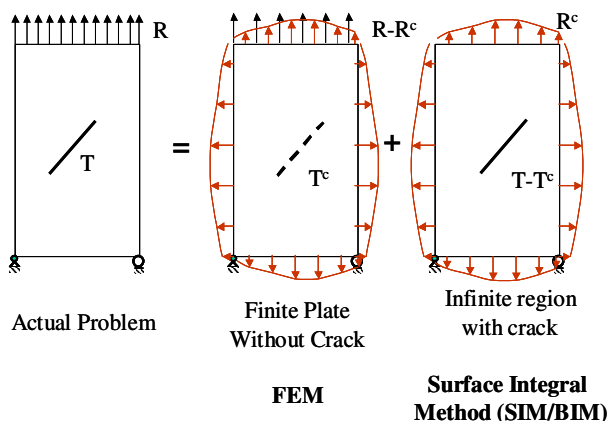
$$T(s) = \int_A \Gamma(r,s) \cdot \delta(r) dA \tag{2}$$

Figure 4 : Schematic of linear superposition.

where T is the generalized traction at point s due to crack opening δ along crack surfaces A and Γ is a fundamental stress-strain solution (Green function). Numerical discretization of this integral equation leads to following matrix equation

$$[C]\{\delta\} = \{T\} - \{T^c\} \tag{3}$$

where $[C]$ is a coefficient matrix relating displacements $\{\delta\}$ to the nodal traction vector $\{T\}$ and coupled with the vector $\{T^c\}$ to satisfy the boundary conditions of the finite element method.

Further, the corrective conditions applied to each method are coupled. This is accomplished by defining $\{R^c\}$ with respect to the surface integral crack opening displacement vector such that

$$\{R^c\} = [G]\{\delta\} \tag{4}$$

where $[G]$ is derived such that the nodal forces are statically equivalent to the surface integral tractions acting on the external surface patches. The traction correction, $\{T^c\}$ is calculated from the finite element solution, and can then be expressed in terms of the finite element nodal displacements as follows

$$\{T^C\} = [S]\{U\} \tag{5}$$

where $[S]$ is derived such that the traction corrections are statically equivalent to the finite element nodal displacements. Finally, the system of equations can be presented in partitioned matrix form such that

$$\begin{bmatrix} K & G \\ S & C \end{bmatrix} \begin{Bmatrix} U \\ \delta \end{Bmatrix} = \begin{Bmatrix} R \\ T \end{Bmatrix} \tag{6}$$

3.2 Generalization of the surface integral method for non-homogeneous materials

In this work, the surface integral method is developed for non-homogeneous materials. The surface integral method numerically models a three-dimensional nonplanar fracture as a continuous distribution of force multipoles. Assuming linear elasticity, one can accurately determine the stresses and displacements induced by a fracture by superimposing the effects of the multipoles. This method has been successfully applied to two- and three-dimensional fracture problems, see Forth and Keat (1998).

The traction vector, $\{T\}$ written in equation (2), induced by a fracture can be represented using indicial notation as

$$t_k = \iint_A \Gamma_{kmn} n_m \delta_n dA \tag{7}$$

where t_k is the traction vector, A is the surface area of the nonplanar fracture, Γ_{kmn} is the stress influence function, n is the normal to the fracture surface, and $\delta_n$gs the crack displacement vector where δ_xg is crack opening, and δ_2, δ_3 are orthogonal components of crack shear.

The bimaterial stress influence functions used in this formulation were developed by Keat, Erguven and Dwyer (1996), starting from Rongved's fundamental solution for point forces near a planar bimaterial interface, see Rongved (1955). The bimaterial influence functions can be decomposed into singular (Γ^S_{kmn}) and nonsingular (Γ^N_{kmn}) terms such that

$$\Gamma_{kmn} = \Gamma^S_{kmn} + \Gamma^N_{kmn} \tag{8}$$

Traction boundary conditions are enforced at collocation points located at the element centroids of a piecewise planar representation of the fracture. In the vicinity of a collocation point, one can subtract off the integral equivalent of a rigid body displacement to reduce the order of the singularity.

$$t_k = \iint_A \Gamma_{kmn} n_m \delta_n dA - \iint_{A_\infty} \Gamma^S_{kmn} n_m \hat{\delta}_n dA \tag{9}$$

where A_∞ is a plane of infinite extent, which is coplanar with the singular element containing the collocation point; and $\hat{\delta}_n$ represents crack opening/shear at the collocation point. Substituting equation (8) into equation (9), the singular element of area A_S can now be integrated in the Cauchy Principal-value sense by arranging terms as follows

$$t_k = \iint_{A-A_S} \Gamma^S_{kmn} n_m \delta_n dA + \iint_{A_S} \Gamma^S_{kmn} n_m (\delta_n - \hat{\delta}_n) dA$$
$$- \iint_{A_\infty - A_S} \Gamma^S_{kmn} n_m \hat{\delta}_n dA + \iint_A \Gamma^N_{kmn} n_m \delta_n dA \tag{10}$$

Discretization of the fracture surface into crack elements leads to the following equivalent form of the traction

equation

$$t_k = \sum_{\substack{i=1 \\ i \neq q}}^{Nele} \iint_{A_i} \Gamma^S_{kmn} n^q_m h_n \hat{\delta}^i_n dA$$

$$+ \iint_{A_q} \Gamma^S_{kmn} n^q_m (h_n - I_n) \hat{\delta}^q_n dA$$

$$+ \oint_{A_q} \mathbf{N}^q \cdot \nabla \phi_{kn} \hat{\delta}^q_n dS + \sum_{i=1}^{Nele} \iint_{A_i} \Gamma^N_{kmn} n^q_m h_n \hat{\delta}^i_n dA \quad (11)$$

where the superscript i indicates crack element correspondence, q identifies the singular crack element containing the collocation point, I_n is the nxn identity matrix, h_n is an interpolation function for crack opening displacements, A_i is the surface area of the ith crack element, and $\mathbf{N}$ is the outward unit normal to the contour enclosing A_q.

It follows from Green's Lemma, see Love (1944), that

$$\Gamma^S_{kmn} n^q_m = \nabla \cdot \nabla \phi_{kn} \quad (12)$$

where Γ^S_{kmn} and ϕ_{kn} are continuously differentiable along the closed contour. Note that the line integral is equivalent to the third term in equation (11) and was introduced to avoid having to discretize the area $A_\infty - A_S$ which is nonsingular and of infinite extent. The remaining area integrals were evaluated using Gauss quadrature.

Local interpolation functions for crack opening were selected based on proximity to the crack front. The interior elements are assumed to have constant crack opening displacements such that $h_n = I_n$. This assumption increases the efficiency of the model and does not degrade the accuracy significantly, see Forth and Keat (1996). A specialized interpolation function was developed for the tip elements using the plane strain elasticity solution. The latter states that the near-tip displacements vary as the square root of the perpendicular distance from the crack front. The general form of the interpolation function for tip elements is defined such that

$$\delta_n = h_n \hat{\delta} \quad \text{and} \quad h_n = \sqrt{\frac{2\rho_n}{\rho_{max}}} \quad (13)$$

where ρ is the perpendicular distance from the crack front and ρ_{max} is the perpendicular distance to the back edge of the tip element under inspection.

3.3 Modeling of interfaces and a finite body

A method for superimposing several half-space solutions to model a bounded geometry was developed by Keat, Maybury and Annigeri (1996). A set of influence functions was introduced for each surface, or bimaterial interface, to model the boundary conditions. Each crack element was then assigned to an interface based on proximity. This procedure alone does not explicitly enforce the boundary conditions of the entire body. Instead, it only captures the first order effects associated with the interface closest to the given crack element. Therefore, a finite element hybridization technique was combined with this method to model the effects of the boundaries not explicitly accounted for by the influence functions.

The method of superposition developed herein varies from the procedure described above, in that all of the interfaces effect the entire crack regardless of proximity. The computational approach taken to model several interfaces, or a layered structure, is to sum the bimaterial influence sets such that equation (11) is written as

$$t_k = \sum_{\substack{i=1 \\ i \neq q}}^{Nele} \iint_{A_i} \Gamma^S_{kmn} n^q_m h_n \hat{\delta}^i_n dA$$

$$+ \iint_{A_q} \Gamma^S_{kmn} n^q_m (h_n - I_n) \hat{\delta}^i_n dA$$

$$+ \oint_{A_q} \mathbf{N}^q \cdot \nabla \phi_{kn} \hat{\delta}^q_n dS$$

$$+ \sum_{i=1}^{Nele} \iint_{A_i} \sum_{j=1}^{Nif} \left[\Gamma^N_{kmn} n^q_m h_n \hat{\delta}^i_n \right] dA \quad (14)$$

where Nif defines the number of interfaces and Γ^N_{kmn} are the nonsingular parts of the influence function, which account for the presence of each interface.

Modeling the effect of all the interfaces on all of the crack elements results in the boundary conditions at all free surfaces and bimaterial interfaces represented simultaneously. Since these boundary conditions are modeled in the surface integral method, the coupling of the finite element and surface integral solutions becomes very weak. Therefore, the correction matrices developed in equations (4) and (5) reduce to approximately zero. Finally, equation (6) can be reduced to

$$\begin{bmatrix} K & 0 \\ 0 & C \end{bmatrix} \begin{Bmatrix} U \\ \hat{\delta} \end{Bmatrix} = \begin{Bmatrix} R \\ T \end{Bmatrix} \quad (15)$$

The finite element solution need not be recomputed with changes in the surface integral model. It is only with large displacements or load redistribution in the system that the two models need to interact to maintain reasonable accuracy. The outcome is that the de-coupling of the models during analysis results in enormous efficiency gains as only the surface integral model is updated during crack propagation.

3.4 Crack propagation

Three-dimensional fracture models, such as the surface integral method, can make use of two-dimensional growth laws by applying them locally along the crack front. This is possible because in the limit as one approaches a three-dimensional crack front, plane strain conditions are approximated. Therefore, the stress intensity factors were computed by substituting tip element displacements into the plane strain definitions given below

$$K_I = \frac{G}{(1-\upsilon)} \frac{\delta_1}{2\sqrt{2\rho/\pi}} \; ; K_{II} = \frac{G}{(1-\upsilon)} \frac{\delta_2}{2\sqrt{2\rho/\pi}} \; ;$$

$$K_{III} = \frac{G\delta_3}{2\sqrt{2\rho/\pi}} \tag{16}$$

where K_I, K_{II}, and K_{III} are the stress intensity factors corresponding to the three fundamental modes, G is the shear modulus and υ is Poisson's ratio specific to the material containing the crack tip element, ρ is the perpendicular distance from the crack front to the collocation point of the element under inspection, and δ_i is the crack opening displacement vector resolved in the local opening, normal, and tangential directions respectively, of the tip element under consideration.

To propagate the crack, both the direction and extension must be computed at each crack tip element. The maximum circumferential stress theory for direction, see Erdogan and Sih (1963), and the Forman fatigue crack growth equation as developed by Forman and Mettu (1992), were applied. Maximum circumferential stress theory determines the direction of crack propagation, θ, by maximizing the circumferential stress at the crack tip such that:

$$K_I \sin\theta + K_{II}(3\cos\theta - 1) = 0 \tag{17}$$

where θ is the angle of growth direction expressed in the local normal-tangential coordinate system of the tip element and K_I and K_{II} are the mode I and mode II stress intensity factors, respectively. The Forman equation was developed to curve fit a large material database that is available through NASA Johnson Space Center and is defined as:

$$\frac{da}{dN} = \frac{C(1-f)^n (\Delta K_{eq})^n (1 - \frac{\Delta K_{th}}{\Delta K_{eq}})^p}{(1-R)^n (1 - \frac{\Delta K_{eq}}{(1-R)K_C})^q} \tag{18}$$

where *da/dN* is the rate of crack growth based on crack length *a* and cycle count *N*; *R* is the stress ratio $\sigma_{min}/\sigma_{max}$; ΔK_{eq} is the equivalent stress intensity factor range which for mixed-mode is defined to be $\Delta K_{eq} = \sqrt{(\Delta K_I)^2 + (\Delta K_{II})^2 + (\Delta K_{III})^2}$ in accordance with the mixed-mode definition of strain energy release rate, see Erdogan (1983) and later Forth, Keat and Favrow (2002); C, n, p and q are empirically derived material constants for each material the crack propagates through; K_c is the fracture toughness and ΔK_{th} is the threshold stress intensity factor range for the material the crack tip element resides in and *f* is the crack opening function.

4 Numerical model calibration

When developing a numerical model, the accuracy of the assumptions that have been made must be evaluated. The following comparisons to respected technical results will address each of the assumptions inherent to the surface integral finite element hybrid method.

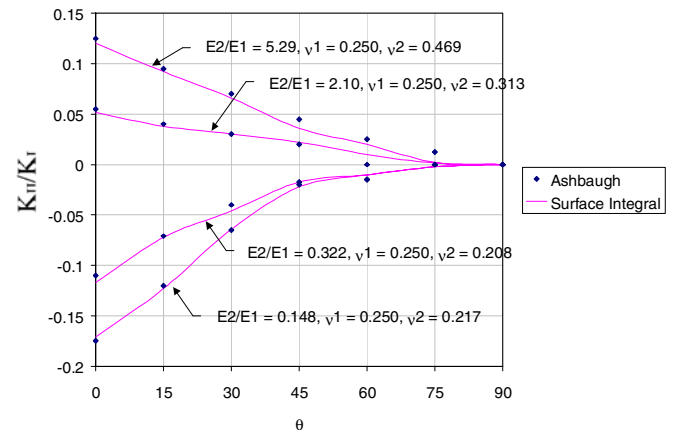### 4.1 Plane strain solution of a crack near an interface

A three-dimensional rectangular crack near a bimaterial interface (13) was modeled using the surface integral method and compared to a two-dimensional plane strain solution by Ashbaugh (1975). The crack was held at a constant 200 elements (10 elements parallel to the interface and 20 elements depth-wise), an aspect ratio of 10, and an *e/a* ratio of 0.4 with both material properties and angle of inclination (θp varied. 4.2 illustrates the level of correlation that was attained for the crack front closest to the material interface.

### 4.2 Plane strain solution of a crack in a composite sandwich

The superposition method can also be applied to bimaterial problems such as a 3D rectangular crack embedded
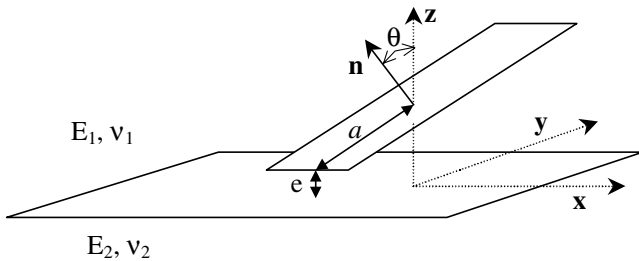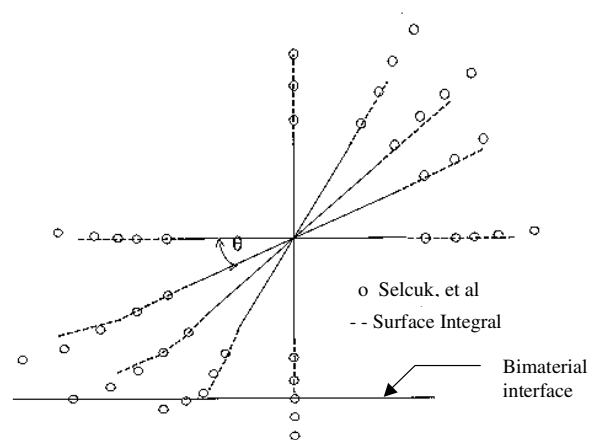
Figure 5 : Definition of a 3D rectangular crack near a planar interface.

Figure 6 : Comparison of results for a 3D rectangular crack near an interface to a 2D plane strain solution. (e/a = 0.4, aspect ratio of crack = 10).
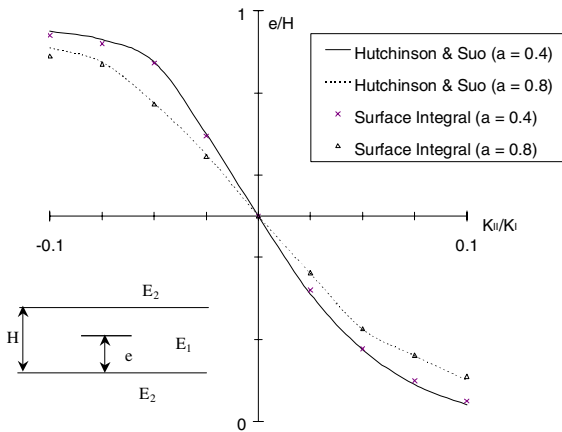
Figure 7 : Stress intensity factor ratio versus crack depth for a crack in a layered material.

Figure 8 : Crack growth trajectories for E2/E1 = 5.

in the middle layer of a composite sandwich (Figure 7). The crack model was held at a constant 200 elements (10 elements across the interior and 20 elements defining the depth), an aspect ratio of 10, and an e/a ratio of 0.4 with the distance between the crack and the interface varied. Figure 7 illustrates good correlation with the 2D solution by Hutchinson and Suo (1992) for two material contrasts (E_2/E_1) of 0.4 and 0.8.

4.3 Growth of a penny-shaped crack towards a bimaterial interface

A penny-shaped flaw initially consisting of 300 elements was propagated towards a planar bimaterial interface, as shown in Figures 8 and 9. The predicted crack trajectory

near the interface is very similar to the two-dimensional results obtained using a boundary element formulation by Selcuk, Hurd, Crouch and Gerberich (1994). However, the crack path predicted using the 3D surface integral model varies slightly from the two-dimensional results away from the interface, especially for large difference between Young moduli. This may be a result of the surface integral formulation having all elements be affected by the bimaterial interface.

5 Application of the Hybrid Numerical Method to the Sensor Design

This numerical method was used to evaluate the feasibility of fabricating an in-situ sensor for real-time detection
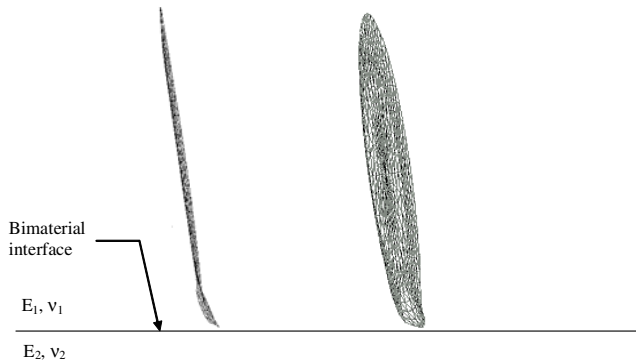
Figure 9 : Growth of a pressurized crack towards an interface (2 views). $E_2/E_1 = 5$, $\nu_1 = \nu_2 = 0.3$ and $\theta = 60$.

Figure 10 : Hybrid Finite element mesh (FEM) and Surface integral mesh (SIM) to predict wired coating failure.

Figure 11 : Hybrid Finite element mesh (FEM) and Surface integral mesh (SIM) to predict wired coating failure. Wires break as the crack in the part propagates.
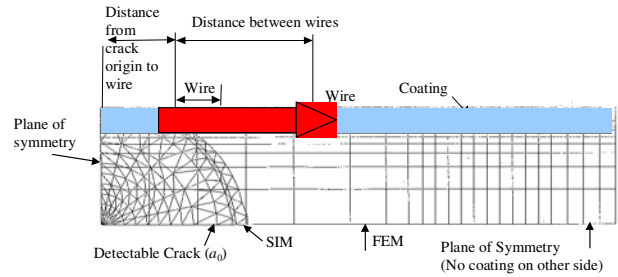
of surface cracks propagating in aircraft engine components. The results of the computations allow us to identify limiting loading conditions and crack configurations for which the crack initially embedded in the part, propagates through the wire mesh without causing delamination of the layered sensor system and in turn generating a false signal.

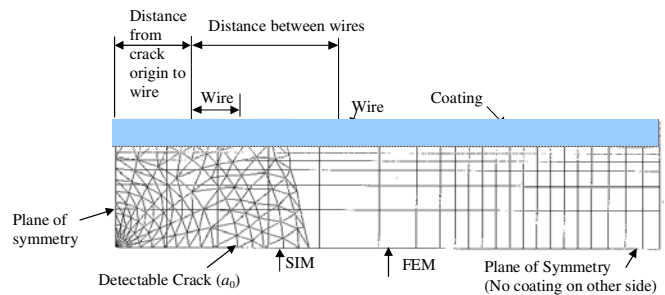### 5.1   Formulation of the Mechanical Problem

The primary stresses incurred in the system are due to disk rotation. Taking into account the axisymmetry of the problem, a constant displacement is applied to both the component and sensor to enforce compatibility. The initial crack was located equidistant between wires such that the wire spacing would be minimized to detect a crack of a_0 as it propagated. Initially, the crack has a penny shape and is completely buried in the base material. While growing, the crack interacts with the sensor coating and will either delaminate (Figure 10) the sensor or become a surface crack (Figure 11). In this section, we numerically study these two crack propagation modes, namely through layer cracking and whole layer delamination.

5.2   Computational Results

Design of the sensor system to withstand the service conditions of a rotating engine component involved determining the principal modes of system failure. The first mode investigated was the catastrophic delamination of the sensor. Initially, the thickness of the coating, c, and the spacing of the wires were varied to determine acceptable stress levels at the component-sensor interface

to avoid rapid delamination. For this study, it was assumed that delamination occurred if the stresses at the interface (K_T) exceeded the mode I fracture toughness (K_{Td}) of the bond similar to the approach outlined in Reeder (2000). Once the onset of delamination was observed, the interface stresses were continually monitored during fatigue crack growth to predict delamination arrest ($K_T/K_{Td} < 1$), stable tearing ($1 < K_T/K_{Td} < 1.5$), or catastrophic failure ($K_T/K_{Td} > 1.5$), see Knappe and Schneider (1973). The trend of a thinner coating producing less delamination stress is clearly illustrated in Figure 12. Also, decreasing the spacing of the wires in the sensor reinforces the system in a manner similar to fibers reinforcing a composite, also depicted in Figure 12. Therefore, the sensor is less prone to delamination if the coating thickness does not exceed 0.166 a_0, and the wire spacing is less than 1.10 a_0. The second mode of failure investigated was fracture of the sensor system due to fatigue cracking of the component. The sensor material is quite brittle, e.g. a lower fracture toughness, K_{T2}, in comparison to the component material, K_{T1}, and will therefore fracture at a lower stress. The key factors
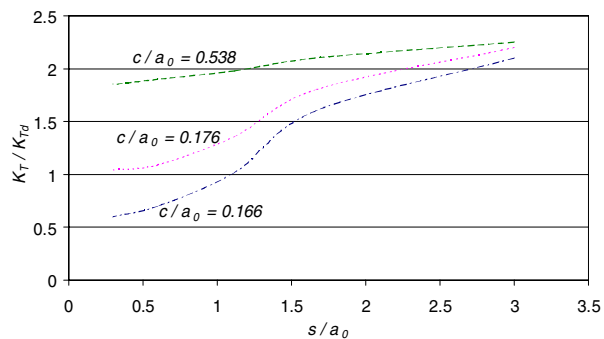
Figure 12 : Effect of coating thickness and wire spacing on delamination.
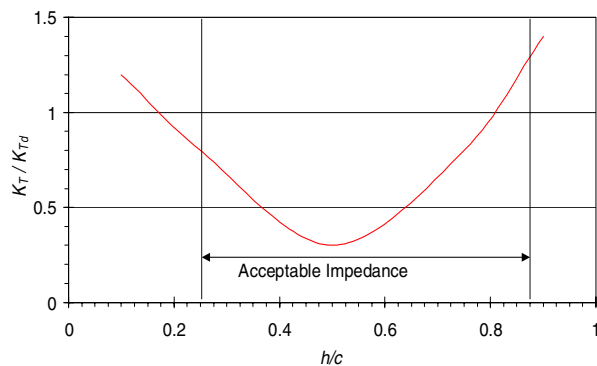
Figure 13 : Effect of wire placement on impedance and initiation of delamination.

in preventing fracture of the sensor are the position of the wire in the mesh and the size of the crack as it approaches the sensor. If the wire is placed too close to the free surface, the insulating layer will simply crack and fall off as the fatigue crack propagates through the part, while the wire remains intact. If the wire is placed too close to the part, then the fatigue crack will break through the insulating layer between the part and the wire causing delamination to occur at the interface. Therefore, the wire in the sensor must be embedded within the coating a minimum of 20% of the coating thickness from either side, as illustrated in Figure 13. This minimum must then be raised to 25% to provide adequate electrical insulation between the component and wire. Two of the numerical analyses are shown representing through-layer cracking (Figure 11) and coating failure (Figure 10).

6   Conclusions

We have developed a novel hybrid numerical method to study three-dimensional crack propagation in a layered structure. We formulated and resolved the problem for a half-space with a thin inhomogeneous-layered surface. The new hybrid method allows direct problem solving without additional correction iterations. The combined usage of the proposed method with crack propagation criteria made possible the incremental growth of three-dimensional non-planar cracks and the prediction of stable and unstable crack propagation.

The completed fracture mechanics modeling has shown that it is possible to design a patterned coating on an aircraft engine rotating part surface which will be adherent at the stresses and temperatures normally present in operation, and will fracture in a controlled manner when, and only when, there is an underlying crack in the disk. The model has predicted an upper boundary of $c/a_0 = 0.175$ for the total coating thickness, of which at least 25% must be the protective layer covering the conductive grid. Although the model predicts improved mechanical performance with thinner insulating and metallic layers, the minimum acceptable thickness is determined by the required electrical properties of the metallic grid. All the electronic concepts studied required that the insulating film between the component and wires be on the order of $c/a_0 = 0.04$ or greater so that the sensor would have an acceptable impedance. Although the work to date has shown that the proposed sensor is viable, many challenges of experimental verification lie ahead before such a sensor can be demonstrated in an operating engine.

References

Curley, R.C.; Fisher, M.; Dileonardi, J.V.; DePinho, A N. (1996): Light weight fan blade containment system. *Applied Science and Manufacturing*, vol. 27, no. 2, pp. 159.

Sturges, D.J. (1994): Role of NDE in predicting residual life for aircraft engine components. *NDT & E International*, vol. 27, iss. 4, pp. 179-184.

Barranger, J.P. (1984): Eddy Current Jet Engine Disk-Crack Monitor. *Materials Evaluation*, vol. 42.

Fahr, A.; Chapman, C. E.; Pelletier, A.; Hay D. R. (1997): Inspection of aircraft engine components using automated eddy current and pattern recognition techniques. *NDT & E International*, vol. 30, iss. 3, pp. 177.

Tietze, M. (1990): New aspects in aircraft inspection using eddy current methods. *AGARD, Impact of Emerging NDE-NDI Methods on Aircraft Design, Manufacture,*

and Maintenance, N90-28068, pp. 22-38.

Brebbia, C. (1978): *The boundary element method for engineers*. Wiley, NY.

Keat, W.D.; Annigeri, B.S.; Cleary, M.P. (1988): Surface integral and finite element hybrid method for two and three dimensional fracture mechanics analysis, *Int. J. of Frac.*, vol. 36, pp. 35-53.

Han; Z.D. and Atluri, S.N. (2002): SGBEM (for Cracked Local Subdomain) – FEM (for uncracked global Structure) Alternating Method for Analyzing 3D Surface Cracks and Their Fatigue-Growth, *CMES: Computer Modeling in Engineering & Sciences*, Vol. 3, No. 6, pp. 699-716.

Han, Z. D. and Atluri, S. N. (2003): Truly Meshless Local Petrov-Galerkin (MLPG) Solutions of Traction & Displacement BIEs, *CMES: Computer Modeling in Engineering & Sciences*, Vol. 4, No. 6, pp. 665-678.

Cruse, T.A. (1988): *Boundary element analysis in computational fracture mechanics*. Kluwer Academic Publishers.

Shifrin E.I.; Staroselsky, A. (2002): A novel method for the solution of the three-dimensional dynamic crack problem. *Damage & Fracture Mechanics. Computer Aided Assessment and Control.* Ed. C. A. Brebbia and S. I. Nishida. WIT Press, pp. 48-54.

Atluri, S.N. (2005): Applications of DTALE: Damage Tolerance Analysis and Life Enhancement [3-D Nonplannar Fatigue Crack Growth], *SID: Structural Integrity & Durability*, Vol. 1, No. 1, pp. 1-20.

Annigeri, B.; Keat W.D.; Cleary, M.P. (1988): Fracture Mechanics Research using the Surface Integral and Finite Element Hybrid Methods. *Proc. of the 1ˢᵗ Japan/US Symposium on BEM*. Univ. of Tokyo, pp. 191-202.

Keat, W.D.; Erguven, M.E.; Dwyer, J.F. (1996): Modeling of 3D mixed-mode fractures near planar bimaterial interfaces using surface integrals. *Int. J. for Num. Meth.*, vol. 39, pp. 3679-3703.

Rongved, R. (1955): Force at a point in the interior of a semi-infinite solid. *Proc. 2nd Midwestern Conf. on Solid Mech.*, pp. 1-13.

Malvern, L.E. (1969): *Intro. To the Mech. of a Continuous Medium*, Prentice-Hall, Englewood Cliffs, N.J.

Mindlin, R.D. (1936): Force at a point in the interior of a semi-infinite solid. *Physics*, vol. **7,** pp. 195-202.

Love, A.E.H. (1944): *A Treatise on Mathematical Theory of Elasticity*. Dover Pub. New York.

Keat, W.D.; Maybury D.M.; Annigeri, B.S.; (1996): Surface integral and finite element hybrid method for three-dimensional analysis of arbitrarily shaped surface cracks. *J. Eng. Gas Turbines & Power,* vol. 118, pp. 406-410.

Reeder, J.R. (2000): Refinements to the mixed-mode bending test for delamination toughness, *Proc. 15ᵗʰ Tech. Conf. Amer. Soc. for Composites*, pp. 991-998.

Erdogan, F.; Sih, G.H. (1963): *ASME J. of Basic Eng.*, vol. 89, pp. 159-525.

Forman, R.G.; Mettu, S.R. (1992): Behavior of Surface and Corner Cracks Subjected to Tensile and Bending Loads in Ti-6Al-4V Alloy. *Fracture Mech.*, 22nd Symposium, vol. 1, ASTM STP 1131, pp. 519-546.

Erdogan, F. (1983): Stress Intensity Factors. *J. Appl. Mech.*, vol. 50, pp. 992-1002.

Auciello, O. (1999): In situ process diagnostics and modeling. *Materials Research Society symposium proceedings*, ISSN02729172, vol. 569.

Elshabini-Riad, A.; Barlow, F.D. (1998): *Thin film technology handbook*, McGraw-Hill, New York.

Lei, J.F.; Martin, L.C.; Will, H.A. (1997): Advances in thin film sensor technologies for engine applications. *NASA-TM-107418.*

Selcuk, S.; Hurd, D.S.; Crouch, S.L.; Gerberich, W.W. (1994): Prediction of interfacial crack path: a direct boundary integral approach and experimental study. *Int. J. of Fracture*, vol. 67, pp. 1-20.

Metev, S.M. (1998): Laser-assisted microtechnology. *Springer series in materials science*, ISSN0933-033X, vol. 19.

Dharan, C.K.H. (1986): Delamination fracture toughness of composite spacecraft structures. *ESA Proceedings of a Workshop on Composites Design for Space Applications*, N86-30758, pp. 159-167.

Forth, S.C.; Keat, W.D. (1998): A 3D Nonplanar Fracture Model for Life Prediction. *Recent Adv. In Mech. of Aerospace Struct. & Mat.*, ASME Press, AD-Vol. 56.

Lu, M.C. (1980): Stress intensity factors in two bonded elastic layers containing cracks perpendicular to and on the interface. NASA-CR-159218.

Keat W.D.; Forth, S.C. (1997): Growth of 3D Curved Cracks Towards a Bimaterial Interface. *Developments in*

Mechanics, vol. 19, pp. 2-7 - 2-9.

Knappe, W.; Schneider, W. (1973): The role of failure criteria in the fracture analysis of fibre-matrix composites. *Deformation and Fracture of High Polymers*, ed. H.H. Kausch, J.A. Hassell and R.I. Jaffee, Plenum Press, New York, pp. 543-556.

Forth, S.C. (1999): Mixed-mode crack growth: An experimental and computational study. *Ph.D. Thesis*, Clarkson University.

Xu, G.; Bower, A.F.; Ortiz, M. (1994): An analysis of nonplanar crack growth under mixed mode loading. *Int. J. Solids & Structures*, vol. 16, pp. 2167-2193.

Guanshui, X.; Argon, A.S.; Ortiz, M.; Bower, A. (1995): Development of a Variational Boundary Integral Method for Analysis of Fully Three Dimensional Crack Advance Problems. *Comp. Mech. '95*, vol. 2, pp. 2874-2889.

Ashbaugh, N. (1975): Stress solution for a crack at an arbitrary angle to an interface. *Int. J. Fracture*, vol. 11, no. 2, pp. 205-219.

Tada, H. (1971): A note on the finite width corrections to the stress intensity factor. *Engng. Frac. Mech.*, vol. 3, no. 3, pp. 345-347.

Hutchinson, J.W.; Suo, Z. (1992): Mixed mode cracking in layered materials. *Adv. In Appl. Mech.*, vol. 29, pp. 63-191.

Forth, S.C.; Keat, W.D. (1996): "Three-dimensional nonplanar fracture model using the surface integral method," *Int. Journal of Fracture*, vol. 77, no. 3, pp 243-262.